Crystallization Behavior of PA66/SiO_2 Organic-Inorganic Hybrid Material

Hua-Lin Wang, Tie-Jun Shi, Shan-Zhong Yang, Lin-Feng Zhai, Guo-Pei Hang

School of Chemical Technology, Hefei University of Technology, Hefei, Anhui, 230009, China

Received 7 June 2004; accepted 20 January 2005
DOI 10.1002/app.22228
Published online in Wiley InterScience (www.interscience.wiley.com).

ABSTRACT: The poly 2-hydroxy propylmethacrylate-methyl methacrylate (PHPMA-MMA)/SiO_2 composite, derived from 2-hydroxy propylmethacrylate (HPMA), methyl methacrylate (MMA), and tetraethoxysilane (TEOS), was used to synthesize polyamide 66(PA66)/SiO_2 organic-inorganic hybrid material. X-ray diffraction (XRD) was used to investigate the lattice spacing change of the PA66/SiO_2 hybrid material. It was found that the addition of PHPMA-MMA/SiO_2 composite nearly did not change the crystal form of PA66. The nonisothermal crystallization kinetics of PA66 and PA66/SiO_2 hybrid material was investigated by differential scanning calorimetry (DSC) with various cooling rates. At every given cooling rate, the start crystallization temperature of the PA66/SiO_2 hybrid material was higher than that of PA66, while the crystallization temperature range was narrower than that of PA66. Avrami analysis modified by the Jeziorny method, the Ozawa method, and a method developed by Liu were employed to describe the nonisothermal crystallization process of the samples. The results showed that the Jeziorny method and the Ozawa method were not suitable to describe the nonisothermal crystallization process of PA66/SiO_2 hybrid material; however, when the relative degree of crystallinity X (t) was less than $1 - 1/e$, $\ln [-\ln (1 - X(t))]$ was still linear to lnt. The Liu method was successful to describe the nonisothermal crystallization processes for both PA66 and the PA66/SiO_2 hybrid material. It was confirmed that the presence of PHPMA-MMA/SiO_2 composite could increase the crystallization rate and had a hetero phase nucleation effect on the PA66 matrix. Moreover, the introduction of PHPMA-MMA/SiO_2 could improve the crystallization active energy $\triangle E$ calculated by the Kissinger equation, attributing to the strong interaction between the polyamide chains and the PHPMA-MMA/SiO_2 composite. J Appl Polym Sci 101: 810–817, 2006

Key words: hybrid material; nonisothermal crystallization kinetics; organic-inorganic; PA66/SiO_2; polyamide 66

INTRODUCTION

Polyamide 66 (PA66), an important engineering plastics with many industrial applications, exhibits high resistance to crack initiation, which imparts high toughness to unnotched materials. However, its high sensitivity to notch propagation under impact leads to embrittlement, which has attracted much attention.[1–4] In recent years, some researches on polyamide/clay nanocomposites have been reported.[5,6] Polyamide/clay nanocomposites also belong to organic-inorganic hybrid materials, which frequently exhibit unexpected hybrid properties synergistically derived from the organic and inorganic components. However, no report to the authors' knowledge is found on the preparation and crystallization behavior of PA66/SiO_2 organic-inorganic hybrid material.

PA66 is a semicrystalline polymer. The major motivation for the formation of the crystal structure in nylons is the strong hydrogen bonds between –NH– groups and –CO– groups. According to the differential spatial arrangement in the hydrogen bonding between the oxygen in the carbonyl group of one polyamide molecular chain and the hydrogen attached to the nitrogen in the neighboring polyamide molecular chain, PA66 has both α and β crystal forms[7] and the α crystal form is more stable than the β crystal form at room temperature.

As we know, crystallization behavior plays a key role in the mechanical properties of semicrystalline polymers. Many works have concerned the study of crystallinity degrees and crystalline transition of polyamides.[8–12] The crystallization behavior is critically dependent on crystallization conditions. It is, therefore, very important to study the crystallization kinetics of PA66/SiO_2 organic-inorganic hybrid material. Polymer crystallization kinetics include isothermal and nonisothermal processes. Compared with the isothermal crystallization process, the nonisothermal crystallization process was more accordable with practice and realized easily. In this experiment, differential scanning calorimetry (DSC) was used to get the nonisothermal crystallization kinetics data by lowering the temperature at a constant rate. Avrami analysis modified by the Jeziorny method, the Ozawa method, and a method developed by Liu were em-

Correspondence to: T.-J. Shi (stjdean@hfut.edu.cn).

ployed to describe the nonisothermal crystallization process.

EXPERIMENTAL

Materials

Tetraethoxysilane (TEOS) with analytical purity ($SiO_2 \geq 28.4\%$) and methyl methacrylate (MMA) with a molecular weight of 100.11 were obtained from the Chemic Medical (Group) Shanghai Chemical Reagent Cooperation. 2-Hydroxy propylmethacrylate (HPMA) with a molecular weight of 144.177 was obtained from the Jilin Chemical Industry Cooperation Suzhou Anli Chemical Plant, Suzhou province, China. The benzoyl peroxide (BPO) used as initiator was purchased from Shandong Laiwu Meixing Chemical Cooperation Limited, Shandong province, China. The Polyamide 66 (PA66) was obtained from the China Shenma Group Nylon66 Salt Cooperation Limited.

Sample preparation

PHPMA-MMA/SiO_2 active sol

Under the catalysis of hydrochloric acid (HCl), TEOS and water (mol ratio of [TEOS]/ [H_2O] = 1 : 2) were hydrolyzed and condensed for 4 h at 45°C in a four-necked round-bottomed flask. Then the protective gas N_2 was lead to the system, and MMA, HPMA (mol ratio of [MMA]/[HPMA]/[TEOS] = 1 : 2 : 4), and the first half of BPO were added; half an hour later, another half of BPO was added, then the temperature was kept constantly at 80°C, and the by product alcohol was removed in time. 6 h later, a transparent homogeneous PHPMA-MMA/SiO_2 active sol was obtained.

PA66/SiO_2 hybrid material

The PHPMA-MMA/SiO_2 active sol and PA66 particles were mixed in a kneader at 80°C for 2 h to cover the PA66 particles with the active sol, then heat treated at 120°C for 8 h in a drier. Finally, the resultant PA66 particles were blended in an extruder and granulated; consequently, the product, PA66/SiO_2 organic-inorganic hybrid material, was obtained.

Measurements

X-ray diffraction analysis (XRD) was carried out to confirm the lattice spacing change of PA66/SiO_2 organic-inorganic hybrid materials. A Japanese D/max-γB rotating diffractometer was employed with the CuK_α radiation source, a tube voltage of 40kV, and tube current of 80mA. Patterns were recorded by monitoring those diffractions that appeared in 2θ from 10° to 35° at a rate of 2°/min.

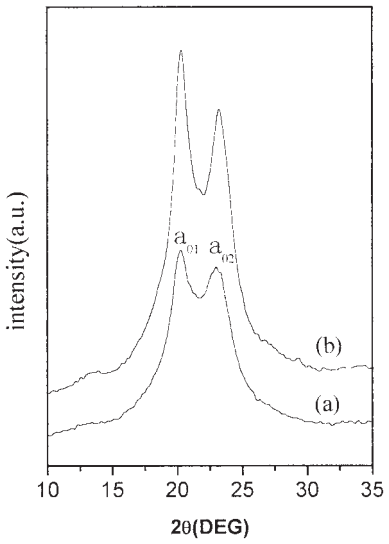

Figure 1 X-ray diffraction scans for samples: (a) PA66 and (b) PA66/SiO_2 hybrid material (1 wt % SiO_2).

Differential scanning calorimetry (DSC) was conducted with a Mettler Toledo DSC-821E under nitrogen atmosphere at a flow of 80 mL/min. For nonisothermal melt-crystallization, the samples were rapidly heated, first to 593K and kept for 10 min in the aluminum crucible to eliminate previous thermal history, then cooled to 413K at constant rates of 5, 10, 20, and 40K/min, respectively. The exothermic crystallization peaks were then recorded and analyzed to estimate the crystallinities under nonisothermal conditions.

RESULTS AND DISCUSSION

X-ray diffraction analysis

PA66 forms chain folded sheets and hydrogen bonds between amide groups of adjacent chains within the sheets. As we know, these chain folded and hydrogen-bonded sheets can stack together, either with a progressive shear, termed the α crystal form, or with an up and down shear, termed the β crystal form. The α crystal form is more stable at room temperature. The two strong diffraction peaks shown in Figure 1 at 2θ = 20.28 and 23.02° are the distinctive features of the α crystal form of PA66, which are designated as α_{01} and α_{02}, respectively. The α_{01} peak arises from the distance between hydrogen-bonded chains, which is the diffraction of hydrogen bonded sheets, while the α_{02} peak arises from the separation of the hydrogen bond sheets.[13] When the PHPMA-MMA/SiO_2 composite was introduced, the XRD pattern of PA66/SiO_2 (1 wt % SiO_2) hybrid material still shows only the presence of the α crystal form shown in Figure 1. However, α_{01} shifted slightly from 20.28 to 20.32° and α_{02} from 23.02 to 23.18°; the *d*-spacing corresponding to the two peaks based on Bragg's equation changed slightly

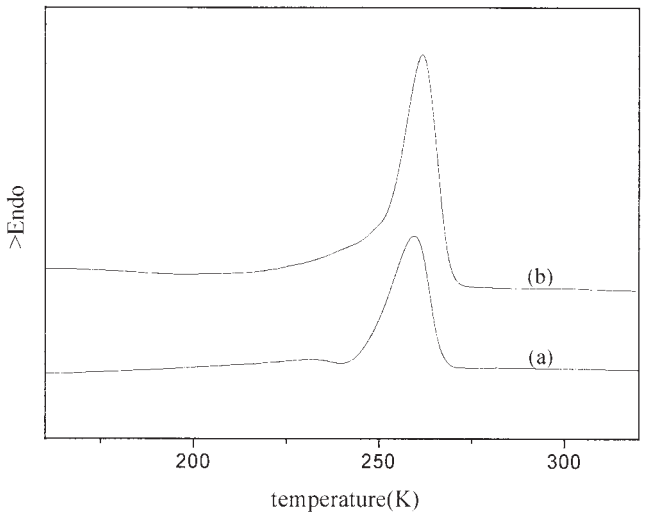

Figure 2 DSC heating scans of samples: (a) PA66 and (b) PA66/SiO_2 hybrid material (1 wt % SiO_2).

from 0.4375 to 0.4366 nm and from 0.3860 to 0.3834, respectively. The active hydroxyl radicals and carbonyl groups of the PHPMA-MMA/SiO_2 composite formed hydrogen bonds with acyl amine bonds, which enhanced the interactions among the chain folded sheets, so the α_{01} and α_{02} peaks shifted slightly to big diffraction angles and the *d*-spacings corresponding to the two peaks were slightly shorted, but the actions were not strong enough to change the crystal form of PA66. Correspondingly, the melt peaks were shifted slightly to higher temperature, shown in Figure 2.

Nonisothermal crystallization kinetics

Crystallization behavior

The crystallization exotherms of PA66 and PA66/SiO_2 hybrid material at various cooling rates are shown in Figure 3. The temperature of the maximum exothermal peak (T_p) shifted to lower temperature with the cooling rate increasing. The reason was that the motion of the PA66 chains could not keep up with the fast cooling rates. Figure 4 illustrates the relations between the start crystallization temperature (T_s) and the cooling rate (ϕ). As shown in Figures 3 and 4, we found that the T_p and T_s of PA66/SiO_2 hybrid material was higher than those of PA66 for a given cooling rate, whereas the crystallization temperature range (R) of PA66/SiO_2 hybrid material was narrower than that of PA66, as can be seen in Figure 5, implying that the addition of PHPMA-MMA/SiO_2 composite had a hetero phase nucleation effect on the PA66 matrix and enhanced the crystallization ability.

Relative degree of crystallinity

The relative degree of crystallinity, $X(t)$, is one of the most important characteristics of polyamide. Moreover, $X(t)$ is the foundation of many isothermal and nonisothermal crystallization kinetic equations.[14–19] To estimate $X(t)$, many analysis equipments are used, such as diffraction scanning calorimetry (DSC), attenuated total reflection (ATR), infrared reflection-absorption infrared spectroscopy (IRRAS), polarization-modulation IRRAS, and so forth.[11] In this experiment, DSC was adapted. $X(t)$ could be defined as:

$$X(t) = \frac{X_c(T)}{X_c(T=\infty)} = \frac{\int_{T_0}^{T} \frac{dH_c(T)}{dT} dT}{\int_{T_0}^{T_\infty} \frac{dH_c(T)}{dT} dT} \quad (1)$$

where $X_c(T)$ and $X_c(T = \infty)$ represented the relative degree of crystallinity at temperature T and the end of

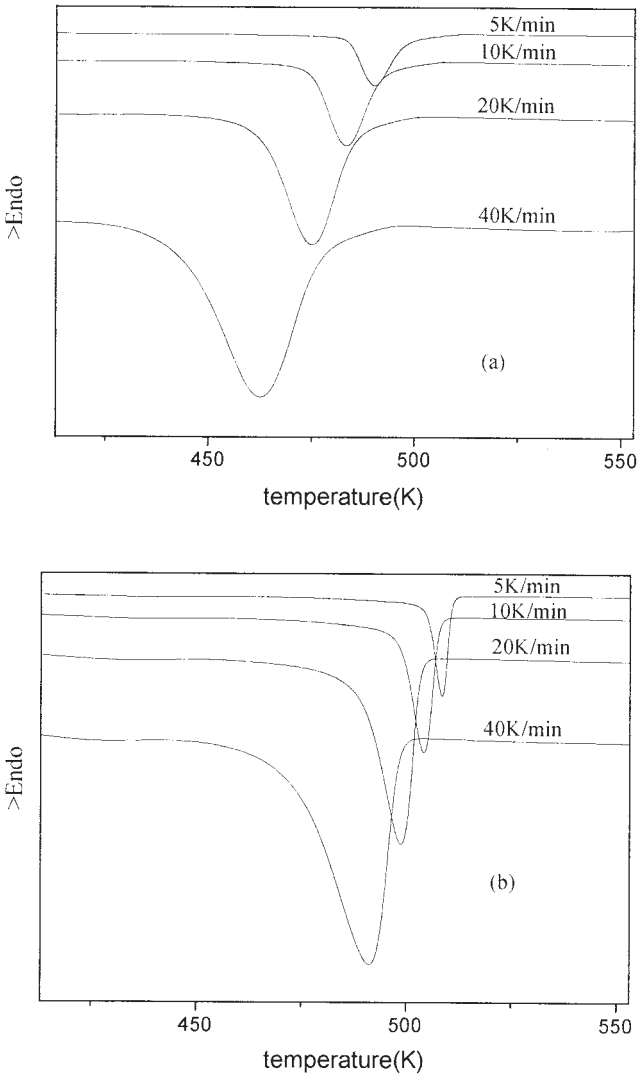

Figure 3 DSC cooling scans of samples: (a) PA66 and (b) PA66/SiO_2 hybrid material (1 wt % SiO_2).

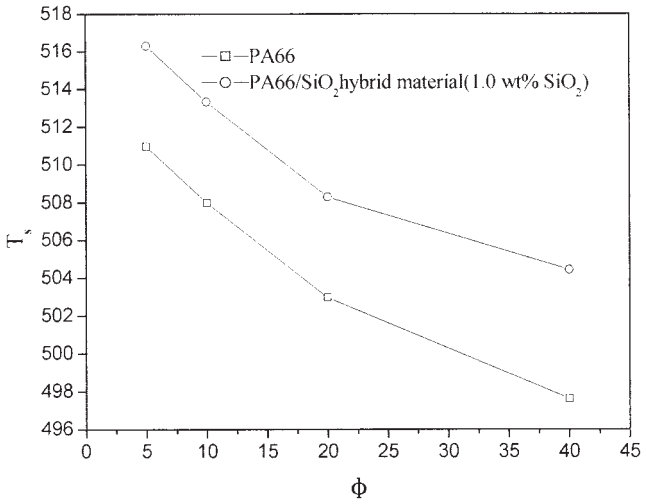

Figure 4 Plots of start crystallization temperature T_s versus cooling rate ϕ.

the crystallization temperature, respectively; T_0 and T_∞ represented the onset and end of the crystallization temperatures, respectively. $X(t)$ could also be defined as:

$$X(t) = \frac{X_c(t)}{X_c(t=\infty)} = \frac{\int_0^t \frac{dH_c(t)}{dt}dt}{\int_0^{t_\infty} \frac{dH_c(t)}{dt}dt} \qquad (2)$$

where $X_c(t)$ and $X_c(t = \infty)$ represented the relative degree of crystallinity at time t and the end of crystallization, respectively. Figure 6 illustrates the relative degree of crystallinity $X(t)$ as a function of temperature for PA66 and PA66/SiO_2 hybrid material based on eq. (1). By the conversion equation $t = (T_0 - T)/\phi$ (T is the temperature at crystallization time t, ϕ is the cooling rate), the horizontal scale could be changed from temperature T (Fig. 6) to time t (Fig. 7), and then X (t) was correspondingly defined as eq. (2).

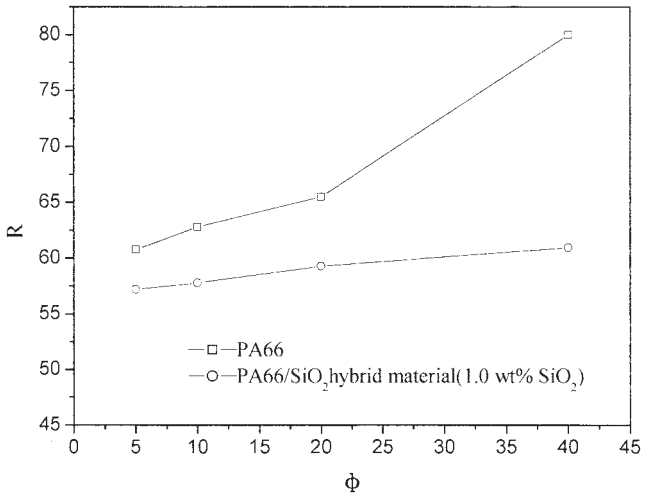

Figure 5 Plots of cooling rate ϕ versus crystallization temperature range R.

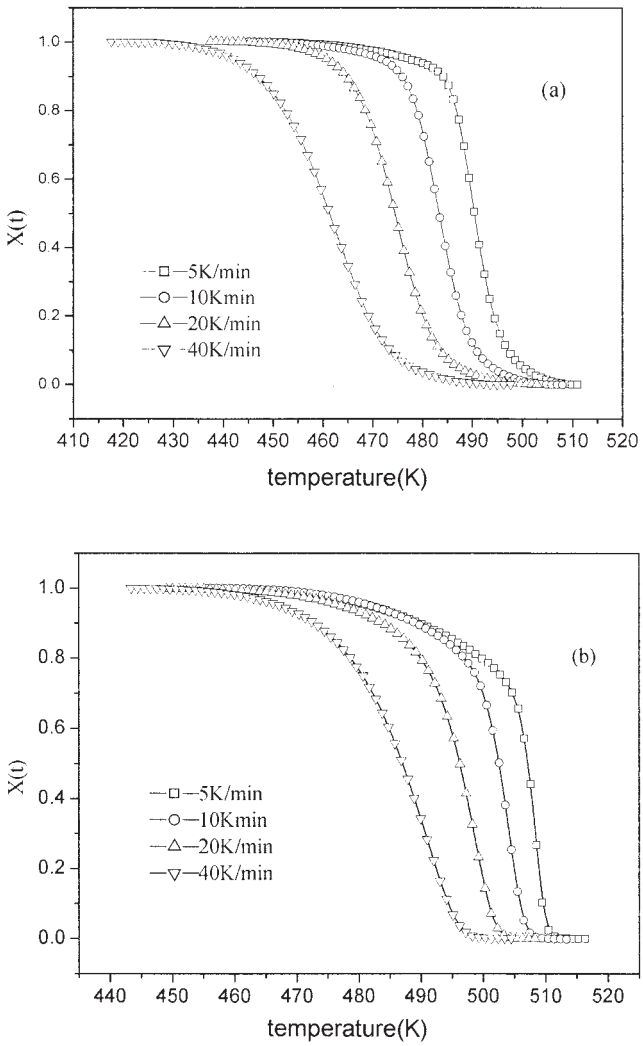

Figure 6 Plots of X (t) versus T during thermal crystallization process: (a) PA66 and (b) PA66/SiO_2 hybrid material (1 wt % SiO_2).

It can be seen that the curves illustrated in Figure 6 shifted to lower temperature with the cooling rate increasing, but all were similar in sigmoid shapes. The phenomenon was caused by the lag effect of the cooling rate during the crystallization process. For the same reason, the half-time of nonisothermal crystallization $t_{1/2}$ obtained from Figure 7 and listed in Table I was shortened gradually with the cooling rate increasing. Moreover, the values of $t_{1/2}$ for PA66 were over two times longer than those of PA66/SiO_2 hybrid material, implying that the presence of PHPMA-MMA/SiO_2 composite could accelerate the overall crystallization process.

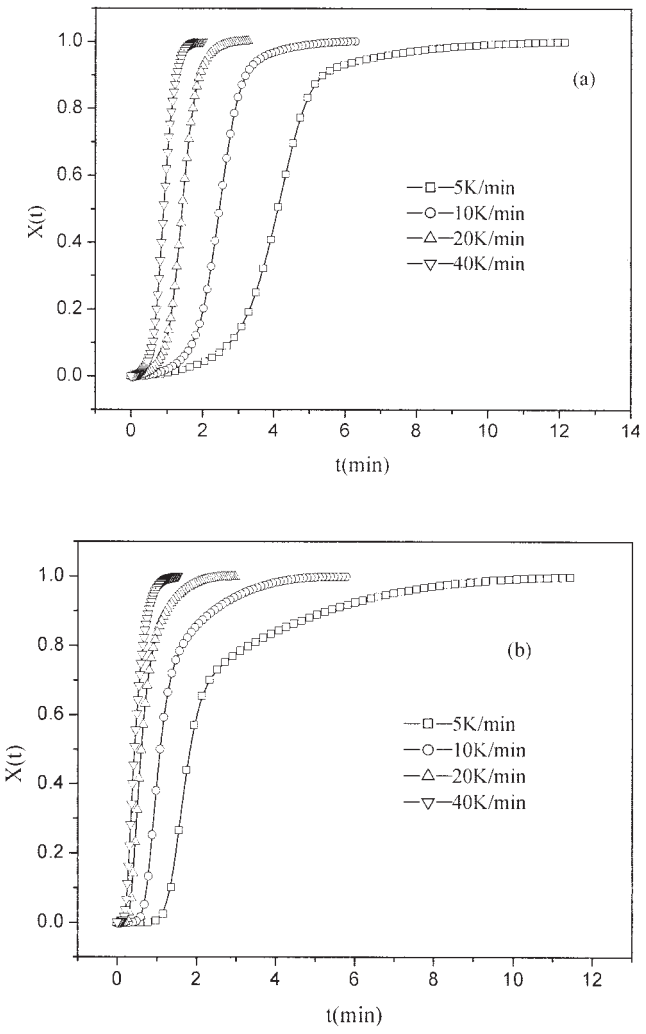

Figure 7 Plots of X (t) versus t during thermal crystallization process: (a) PA66 and (b) PA66/SiO_2 hybrid material (1 wt % SiO_2).

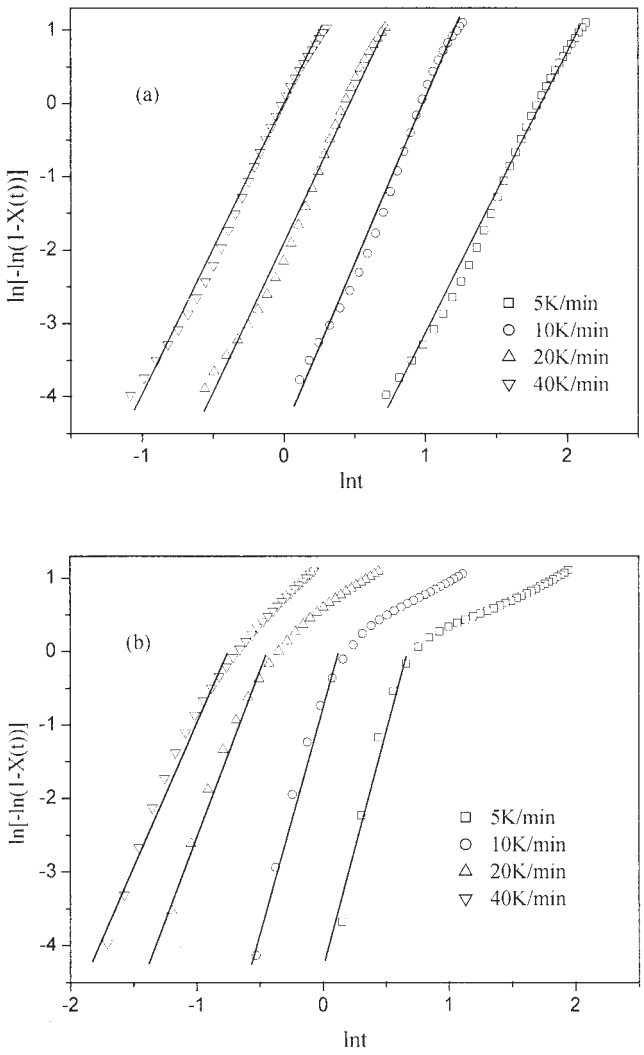

Figure 8 Plots of ln [− ln (1 − X (t))] versus lnϕ during thermal crystallization process: (a) PA66 and (b) PA66/SiO_2 hybrid material (1 wt % SiO_2).

Jeziorny method

The Avrami equation[14] was effectively used in isothermal crystallization kinetics researches.

TABLE I
Nonisothermal Crystallization Kinetic Parameters for PA66 and PA66/SiO_2 Hybrid Material

Sample	Φ (K/min)	T_p	$T_{1/2}$ (min)	n	Z_c
PA66	5	490.46	4.08	3.83	0.25
	10	482.90	2.46	4.46	0.64
	20	475.34	1.41	4.06	0.91
	40	461.66	0.89	3.88	1.00
PA66/SiO_2 Hybrid material (1wt % SiO_2)	5	508.53	1.81	6.60*	0.43*
	10	504.13	1.04	6.10*	0.93*
	20	498.27	0.58	4.52*	1.11*
	40	491.44	0.42	4.03*	1.10*

*$X(t) < 1 - 1/e$.

$$\ln[-\ln(1-X(t))] = \ln Z_t + n\ln t \quad (3)$$

where $X(t)$ is the relative degree of crystallinity at time t, Z_t the crystal growth constant, and n the Avrami exponent depending on the nucleation mechanism and the dimension of the crystal growth. Jeziorny adapted the Avrami equation to describe the nonisothermal crystallization process. Considering the nonisothermal crystallization character, the crystal growth constant Z_t was revised by Z_c with the following equation[15]:

$$\ln Z_c = \ln Z_t/\phi \quad (4)$$

where ϕ is the cooling rate. Figure 8 illustrates the plots of ln [− ln (1 − X (t))] against ln$t$ (min) for each cooling rate. The results showed that the Avrami equation was suitable to describe the nonisothermal

crystallization process of PA66, but was not suitable for PA66/SiO_2 hybrid material. It was interesting that when the PA66/SiO_2 hybrid material was at a low relative degree of crystallinity $X(t) < 1 - 1/e$, the ln [− ln (1 − X (t))] was linear to lnt. The crystallization kinetic parameters obtained from Avrami Z_c plots and the Jeziorny method are listed in Table I. As can be seen in Table I, the Avrami exponent n for PA66 was larger than that of the PA66/SiO_2 hybrid material at every cooling rate, showing that the PHPMA-MMA/SiO_2 composite acted as a hetero phase nucleation agent and changed the nucleation mechanism. Moreover, compared to PA66, the crystal growth constant Z_c of PA66/SiO_2 hybrid material at every cooling rate was larger than that of PA66 at X (t) $< 1 - 1/e$, implying the addition of PHPMA-MMA/SiO_2 composite could accelerate the overall crystallization process of PA66/SiO_2 hybrid material.

Ozawa method

Based on the Evans theory, Ozawa deduced the crystallization kinetic equation of polymers in a nonisothermal crystallization process as follows:[16]

$$\ln[-\ln(1 - X(t))] = \ln P(T) - m\ln\phi \tag{5}$$

where $X(t)$ is the relative degree of crystallinity at time t, m the Ozawa exponent depending on the dimension of the crystal growth, and ϕ the cooling rate. $P(T)$ is the function of temperature depending on the nucleation mechanism, nucleation rate, crystal growth constant, and so forth. Plotting ln [− ln (1 − $X(t)$)] against lnϕ at a given temperature, the curves shown in Figure 9 were obtained. It was clearly seen that the curves for PA66 exhibited a linear relationship, but for PA66/SiO_2 hybrid material, the curves were nonlinear. That is to say, the Ozawa method was valid for PA66 and invalid for PA66/SiO_2 hybrid material.

Liu method

Combining the Ozawa method with Avrami equations, Liu obtained a new method to describe nonisothermal crystallization, and the following equation was obtained:[17]

$$\ln\phi = \ln F(T) - a\ln t \tag{6}$$

where $F(T) = [K(T)/Z_t]^{1/m}$ and refers to the cooling rate that must be chosen within a crystallization time unit when the measured system crystallizes to a certain degree. a = n/m, the ratio of the Avrami exponent n to the Ozawa exponent m. As can be seen in Figure 10, a linear relation between lnϕ and lnt was observed. The kinetic parameters $F(T)$ and a determined from the intercept and slope of the lines are listed in Table II. The value of $F(T)$ for PA66 was much bigger than that for PA66/SiO_2 hybrid material, indicating PA66/SiO_2 hybrid material crystallized more quickly than PA66, which was in conformity with the conclusions drawn from the Jeziorny method.

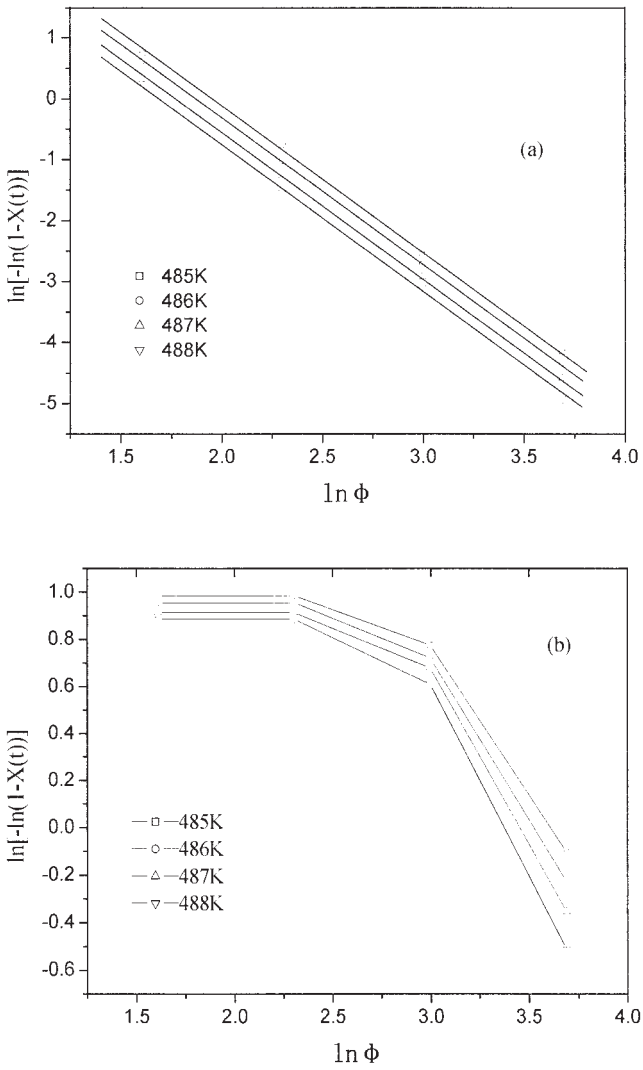

Figure 9 Plots of ln [− ln (1 − X (t))] versus lnt during thermal crystallization process: (a) PA66 and (b) PA66/SiO_2 hybrid material (1 wt % SiO_2).

Kissinger method

The Kissinger equation[20] as follows could be used to describe the crystallization process on condition that the relationship between the crystallization rate and the temperature agreed with the Arrhenius equation.

$$\frac{d\left(\ln\frac{\phi}{T_p^2}\right)}{d\left(\frac{1}{T_p}\right)} = -\frac{E_d}{R} \tag{7}$$

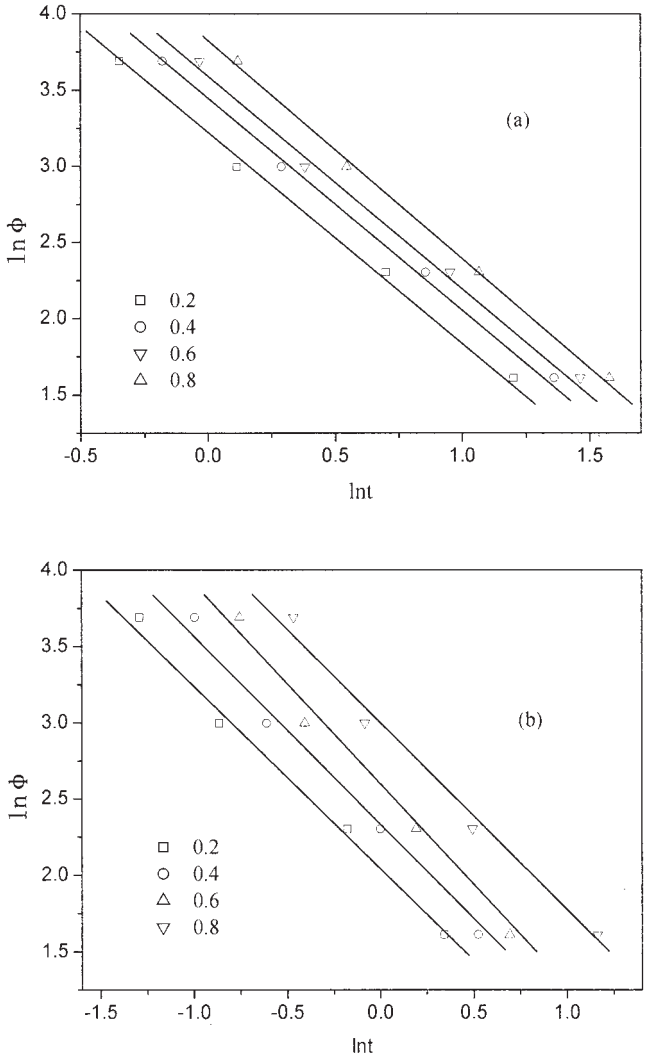

Figure 10 Plots of lnϕ versus lnt during thermal crystallization process: (a) PA66 and (b) PA66/SiO_2 hybrid material (1 wt % SiO_2).

where T_p was the temperature at the maximum crystallization peak and E_d the crystallization active energy. Plots of ln (ϕ /T^2) against 1/T of PA6 and

TABLE II
Nonisothermal Crystallization Kinetic Parameters for PA6 and PA6/SiO_2 Hybrid Materials

Sample	X(t)	a	F(T)	ΔE(kJ/mol)
PA66	0.2	1.40	25.03	150.8
	0.4	1.40	31.50	
	0.6	1.40	36.23	
	0.8	1.43	45.60	
PA66/SiO_2 hybrid material (1wt % SiO_2)	0.2	1.21	7.75	248.82
	0.4	1.23	10.27	
	0.6	1.31	13.46	
	0.8	1.22	20.08	

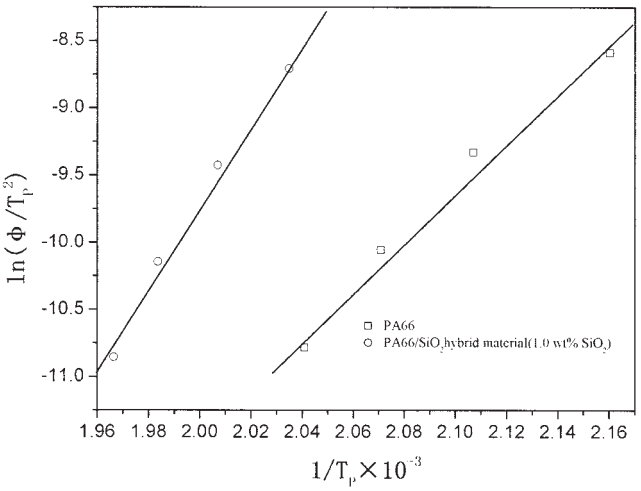

Figure 11 Plots of ln (ϕ /T_p^2) versus 1/T_p for PA66 and PA66/SiO_2 hybrid material.

PA6/SiO_2 hybrid material were made. The crystallization active energy E_d determined from the slope of the lines shown in Figure 11 is listed in Table II. As can be seen, the value of E_d for PA66 is smaller than that for PA6/SiO_2 hybrid material, indicating the addition of PHPMA-MMA/SiO_2 composite improved the crystallization active energy.

CONCLUSIONS

The addition of PHPMA-MMA/SiO_2 composite nearly did not change the crystal form of PA66, but had a hetero phase nucleation effect on the PA66 matrix and enhanced the crystallization ability, which shortened the crystallization time and temperature range, and increased the start crystallization temperature. The Jeziorny method and the Ozawa method were suitable to describe the nonisothermal crystallization process of PA66 and unsuitable for PA66/SiO_2 hybrid material, but when X (t) was less than $1 - 1/e$, ln [$-$ ln $(1 - X(t))$] was linear to lnt for PA66/SiO_2 hybrid material. The Liu method was successful in describing the nonisothermal crystallization processes for both PA66 and PA66/SiO_2 hybrid material. Attributing to the strong interaction between polyamide chains and surfaces of PHPMA-MMA/SiO_2 composite, the presence of PHPMA-MMA/SiO_2 composite improved the crystallization active energy calculated by the Kissinger equation.

The authors gratefully acknowledge financial support from the National Nature Science Foundation of China (grant no. 20174007).

References

1. Harmia, T.; Friedrich, K. Compos Sci Technol 1995, 53, 423.
2. Harmia, T.; Friedrich, K. Plast Rubber Compos Process Appl 1995, 23, 63.

3. Huang, C. C.; Chang, F. C. Polym 1997, 38, 4287.
4. Muratoğlu, O. K.; Argon, A. S.; Cohen, R. E.; Weinberg, M. Polym 1995, 36, 4771.
5. Liu, Q.; Zhao, Z. D.; Ou, Y. H.; Qi, Z. N.; Wang, F. S. Acta Polym Sinica China 1997, 2, 188.
6. Liu, X. H.; Wu, Q. J.; Berglund, L. A. Polym 2002, 43, 4967.
7. Bunn, C. W.; Garner, E. V. Proc R Soc London 1947, 189A, 39.
8. Vasanthan, N.; Salem, D. R. J Polym Sci 1999, 38, 516.
9. Polizzi, S.; Fagherazzi, G.; Benedetti, A.; Battagliarin, M. J Eur Polym 1991, 27, 85.
10. Mo, Z.; Yang, B.; Zhang, H. Anal Sci 1991, 7, 1637.
11. Elzein, T.; Brogly, M.; Schultz, J. Polym 2002, 43, 4811.
12. Li, Y. J.; Yan, D. Y.; Zhu, X. Y. Macromol Rapid Commun 2000, 21, 1282.
13. Vasanthan, N.; Murthy, N. S.; Bray, R. G. Macromolecules 1998, 31, 8433.
14. Avrami, M. J Chem Phys 1941, 9, 177.
15. Jeziorny, A. Polymer 1978, 19, 1142.
16. Ozawa, T. Polymer 1971, 12, 150.
17. Liu, T. X.; Mo, Z. S.; Wang, S. E.; Zhang, H. F. Polym Eng Sci 1997, 37, 568.
18. Harnish, K.; Muschik, H. Colloid Polym Sci 1983, 261, 908.
19. Dutta, A. Polym Commun 1990, 31, 451.
20. Kissinger, H. E. Anal Chem 1957, 29, 1702.